

# Apparent Intracellular $Mg^{2+}$ Buffering in Neurons of the Leech *Hirudo medicinalis*

D. Günzel, F. Zimmermann, S. Durr, and W.-R. Schlue

Institut für Neurobiologie, Heinrich-Heine-Universität Düsseldorf, D-40225 Düsseldorf, Germany

**ABSTRACT** The apparent intracellular  $Mg^{2+}$  buffering, or muffling (sum of processes that damp changes in the free intracellular  $Mg^{2+}$  concentration,  $[Mg^{2+}]_i$ , e.g., buffering, extrusion, and sequestration), was investigated in Retzius neurons of the leech *Hirudo medicinalis* by iontophoretic injection of  $H^+$ ,  $OH^-$ , or  $Mg^{2+}$ . Simultaneously, changes in intracellular pH and the intracellular  $Mg^{2+}$ ,  $Na^+$ , or  $K^+$  concentration were recorded with triple-barreled ion-selective microelectrodes. Cell volume changes were monitored measuring the tetramethylammonium (TMA) concentration in TMA-loaded neurons. Control measurements were carried out in electrolyte droplets (diameter 100–200  $\mu m$ ) placed on a silver wire under paraffin oil. Droplets with or without ATP, the presumed major intracellular  $Mg^{2+}$  buffer, were used to quantify the pH dependence of  $Mg^{2+}$  buffering and to determine the transport index of  $Mg^{2+}$  during iontophoretic injection. The observed pH dependence of  $[Mg^{2+}]_i$  corresponded to what would be expected from  $Mg^{2+}$  buffering through ATP. The quantity of  $Mg^{2+}$  muffling, however, was considerably larger than what would be expected if ATP were the sole  $Mg^{2+}$  buffer. From the decrease in  $Mg^{2+}$  muffling in the nominal absence of extracellular  $Na^+$  it was estimated that almost 50% of the ATP-independent muffling is due to the action of  $Na^+/Mg^{2+}$  antiport.

## INTRODUCTION

It is a well established fact that intracellular free  $Mg^{2+}$  concentrations ( $[Mg^{2+}]_i$ ) are considerably lower than total intracellular  $Mg^{2+}$  concentrations ( $[Mg]_i$ ). In fact, 90–95% of the intracellular  $Mg^{2+}$  is believed to be either bound to intracellular compounds, especially to ATP, or sequestered within intracellular organelles, such as mitochondria or the sarcoplasmic reticulum (for review see Romani and Scarpa, 1992). Due to the equilibrium between free and bound/sequestered  $Mg^{2+}$  and because  $Mg^{2+}$  is constantly transported across the cell membrane by various influx and efflux pathways, changes in  $[Mg^{2+}]_i$  as measured with ion-selective microelectrodes or fluorochromes mirror only part of the actual changes in  $[Mg]_i$ .

The need to distinguish between the pure chemical buffering of intracellular ions and an apparent buffering caused by influx, efflux, and/or sequestration to understand ion homeostasis was recognized some 30 years ago, initially with regard to  $H^+$  (Siesjö and Sørensen, 1971) followed by  $Ca^{2+}$  (Thomas et al., 1991; Schwiening and Thomas, 1996). Thomas et al. (1991) coined the term muffling to describe the multitude of processes that damp changes in free intracellular ion concentrations, while pointing out that the term buffering should only be used for ion chelation by buffers (Schwiening and Thomas, 1996). This terminology is adopted in the present paper. An important difference between buffering and muffling is the time dependence of the

latter, as both ion sequestration and extrusion are slow compared with buffering processes (Siesjö and Sørensen, 1971).

$Mg^{2+}$  muffling has been reported to depend on the intracellular pH ( $pH_i$ ). This is usually attributed to the pH dependence of  $Mg^{2+}$  binding to ATP (Freudenrich et al., 1992; Grubbs and Walter, 1994; Li and Quamme, 1994; Rajdev and Reynolds, 1995). While the apparent dissociation constant ( $K_{ATP}$ ) for  $Mg^{2+}$  binding to ATP is almost constant at pH values above 7.0, it increases considerably at more acidic values (Günzel et al., 1997; Lüthi et al., 1999). Thus, increases in  $[Mg^{2+}]_i$  are to be expected under conditions that elicit strong intracellular acidification, such as ischemia (for review see Lipton, 1999).

Other possibilities for interactions between  $[Mg^{2+}]_i$  and  $pH_i$  should, however, be kept in mind. Mechanisms that transport  $Mg^{2+}$  across the cell membrane may directly or indirectly be influenced by changes in pH. Direct effects are likely to occur in preparations in which  $Mg^{2+}$  transport is coupled to the transport of  $H^+$  or  $HCO_3^-$  ( $Mg^{2+}/H^+$  antiport, distal colon of the rat, Scharrer and Lutz, 1990; ruminal epithelial cells, Leonhard-Marek et al., 1998;  $Mg^{2+}$ - $HCO_3^-$  cotransport, ascites tumor cells, Günther et al., 1986). Indirect effects may be caused by changes in the  $Na^+$  gradient in those preparations in which the transport both of  $H^+$  and of  $Mg^{2+}$  is coupled to a  $Na^+$  antiport (Günzel and Schlue, 1997).

Changes in  $pH_i$  may also influence  $Mg^{2+}$  uptake into/release from mitochondria, as mitochondria have been reported to extrude  $Mg^{2+}$  via a  $Mg^{2+}/H^+$  antiport (Jung and Brierley, 1994). In addition,  $Mg^{2+}$  may be released from mitochondria during an alkalization of the mitochondrial matrix (Günzel et al., 1997, 1999), possibly through activation of the mitochondrial permeability transition pore.

Received for publication 2 August 1999 and in final form 12 December 2000.

Address reprint requests to Dr. D. Günzel, Institut für Neurobiologie, Heinrich-Heine-Universität Düsseldorf, Universitätsstrasse 1, Geb. 26.02, D-40225 Düsseldorf, Germany. Tel.: 49-211-811-4252; Fax: 49-211-811-3415; E-mail: guenzel@uni-duesseldorf.de.

© 2001 by the Biophysical Society

0006-3495/01/03/1298/13 \$2.00

Various approaches have been used to investigate intracellular  $Mg^{2+}$  buffering/muffling: titration of  $[Mg^{2+}]_i$  in erythrocytes that were either permeabilized with the ionophore A23187 (Flatman and Lew, 1980; Flatman, 1988; Raftos et al., 1999) or lysed to obtain a cytoplasmic fraction (Günther et al., 1995), pressure injection of  $Mg^{2+}$  into muscle fibers (Westerblad and Allen, 1992), activation of an intrinsic  $Mg^{2+}$  influx pathway in muscle fibers (Csernoch et al., 1998), and release of  $Mg^{2+}$  bound to ATP by inhibition of the cell metabolism in cardiomyocytes (Koss et al., 1993; Koss and Grubbs, 1994) and in cells of a smooth muscle cell line (BC<sub>3</sub>H-1, Grubbs and Walter, 1994). The multitude of definitions used to describe  $Mg^{2+}$  buffering in these publications makes it difficult to compare the values obtained. However, despite the differences in the preparations and methods used, most of these investigations indicate that, apart from ATP, there is at least one additional pool of cytoplasmic  $Mg^{2+}$  buffers with a large capacity (buffer concentration between ~8 and 20 mM) and a low affinity ( $K_{app} \sim 1$ –3 mM).

The investigations presented here are an attempt to quantify intracellular  $Mg^{2+}$  muffling and its pH dependence in Retzius neurons of the medicinal leech. The experimental approach was an iontophoretic injection of the respective ions,  $Mg^{2+}$ ,  $H^+$ , and  $OH^-$  into these neurons and, for comparison, into electrolyte droplets of a defined composition. The changes in  $pH_i$  and  $[Mg^{2+}]_i$ , the intracellular  $Na^+$  concentration ( $[Na^+]_i$ ), or the intracellular  $K^+$  concentration ( $[K^+]_i$ ) were recorded simultaneously with triple-barreled ion-selective microelectrodes. To exclude the possibility that the observed effects were distorted by cell volume changes, neurons were loaded with tetramethylammonium (TMA) and the intracellular concentration of TMA ( $[TMA]_i$ ) was measured with TMA-sensitive microelectrodes. As previously shown, changes in  $[TMA]_i$  are inversely proportional to changes in cell volume (Dierkes et al., 2001).

Some of the results presented here have been published in abstract form (Günzel et al., 1998).

## MATERIALS AND METHODS

### Preparation and bath solutions

Experiments were carried out on Retzius neurons of the leech *Hirudo medicinalis*. Segmental ganglia from the leech central nervous system were dissected as described by Schlue and Deitmer (1980). Single ganglia were transferred to an experimental chamber and fixed ventral side up by piercing the connectives with insect pins. The chamber had a volume of ~200  $\mu$ l and was continuously perfused with saline at a rate of ~5 ml  $min^{-1}$  at room temperature (20–25°C). The standard leech saline contained (in mM) 85 NaCl, 4 KCl, 2 CaCl<sub>2</sub>, 1 MgCl<sub>2</sub>, 10 HEPES, pH 7.4 adjusted with NaOH. For a nominally  $Mg^{2+}$ -free saline, MgCl<sub>2</sub> was omitted without substitution. A nominally  $Na^+$ -free solution was obtained by an equimolar substitution of  $Na^+$  with *N*-methyl-D-glucamine (NMDG<sup>+</sup>).

### Ion-selective microelectrodes

Double- and triple-barreled microelectrodes were pulled from borosilicate glass capillaries (double-barreled, TGC200–15 or GC150F-15 and GC100F-15; triple-barreled, TGC200–15 and GC150F-15; Clark, Reading, UK), silanized, and filled with ion sensors for  $Mg^{2+}$ ,  $Na^+$ ,  $K^+$ , TMA (used as a tracer of changes in cell volume), and/or pH ( $Mg^{2+}$  sensor ETH 5214, cocktail IIa;  $Na^+$  sensor ETH 227, cocktail Ia;  $K^+$  sensor valinomycin; and pH sensor ETH 1907, cocktail IIa (FLUKA, Buchs, Switzerland) and the ion exchanger Corning 477317 as a sensor for TMA) as described by Günzel and Schlue (1996) and Dierkes et al. (2001). The electrodes were back-filled with 100 mM MgCl<sub>2</sub>, NaCl, and KCl for  $Mg^{2+}$ -,  $Na^+$ -, and  $K^+$ - or TMA-sensitive barrels, respectively. pH-sensitive barrels were back-filled with the pH 7.67 calibration solution (for composition see below). One barrel of each microelectrode was filled with 3 M KCl or, in case of the  $K^+$  and TMA electrodes, with 3 M LiOAc plus 8 mM KCl and served as an intracellular reference. Membrane potentials ( $E_m$ ) measured with LiOAc-filled electrodes were not significantly different from those measured with KCl-filled electrodes.

All potentials were measured against the potential of an extracellular reference electrode (agar bridge containing 3 M KCl and an Ag/AgCl cell), using voltmeters with an input resistance of  $10^{15} \Omega$  (FD223, WPI, Berlin, Germany). The output signals were AD-converted and continuously recorded on a PC. The pure ionic potentials (difference between the potentials of the ion-sensitive barrels and the reference barrel) were obtained directly by means of the built-in differential amplifier of the electrometer.

Before and after every experiment, the  $Na^+$ - and  $Mg^{2+}$ -sensitive barrels of the microelectrodes were calibrated as described by Günzel et al. (1997). The pH-sensitive barrels were calibrated in solutions containing an ionic background of (in mM) 110 KCl, 10 NaCl, 0.5 MgCl<sub>2</sub>. To this solution either 10 mM HEPES was added, when buffered to a pH of 7.67, or 10 mM 2-[*N*-morpholino]ethanesulfonic acid (MES), when buffered to pH values of 6.22 and 5.5. All pH values were adjusted with KOH.

Electrodes filled with valinomycin were calibrated in solutions containing ratios of KCl/NaCl (in mM) of 100:0, 25:75, 5:95, and 0:100 in addition to 0.5 mM MgCl<sub>2</sub> and 10 mM HEPES at a pH of 7.3, adjusted with NaOH. The electrodes based on Corning 477317 were virtually insensitive to changes in  $K^+$  concentration in the presence of  $\geq 1$  mM TMA (Dierkes et al., 2001). TMA could therefore be used as a tracer of changes in cell volume, even if the intracellular  $K^+$  concentration changed substantially. TMA-electrodes were calibrated in solutions containing (in mM) 10, 2.5, 0.5, and 0 TMA, respectively, at an ionic background of 80 KCl, 0.5 MgCl<sub>2</sub>, 10 HEPES, pH 7.3 adjusted with NaOH. As previously demonstrated, cross-talk between the ion-sensitive barrels of triple-barreled microelectrodes was minimal (Günzel et al., 1997; Hintz et al., 1999) and the observed changes in  $pH_i$  and  $[Na^+]_i$  did not cause interference at the  $Mg^{2+}$ -sensitive barrel (see, e.g., Fig. 1 in Günzel et al., 1997).

Electrodes were used if their slope in the linear range of the electrode was at least 80% of the Nernstian slope and if their detection limit was below the values recorded during an experiment. Slopes and detection limits were (mean  $\pm$  SD):  $-30.8 \pm 4.6$  mV/pMg-unit and  $0.1 \pm 0.06$  mM for 34  $Mg^{2+}$ -sensitive barrels,  $-46.8 \pm 0.9$  mV/pNa-unit and  $1.2 \pm 0.12$  mM for 10  $Na^+$ -sensitive barrels,  $-55.0 \pm 1.7$  mV/pK-unit and  $0.05 \pm 0.03$  mM for 4  $K^+$ -sensitive barrels,  $-56.1 \pm 3.2$  mV/pTMA-unit and  $0.09 \pm 0.03$  mM for 6 TMA-sensitive barrels, and  $-53.9 \pm 3.1$  mV/pH-unit for 38 pH-sensitive barrels. Electrodes were calibrated before and after every experiment. As previously described (Günzel et al., 1997; Hintz et al., 1999), these two calibration curves usually were in good agreement for  $Na^+$ -,  $K^+$ -, TMA-, and pH-sensitive barrels, whereas  $Mg^{2+}$ -sensitive barrels initially often showed super-Nernstian slopes and suffered from considerable loss in sensitivity during an experiment. An experiment was used for quantitative evaluation only if the  $[Mg^{2+}]_i$  values calculated from the two calibration curves did not differ by more than 0.4 mM (Günzel et al., 1997; Hintz et al., 1999).

Means  $\pm$  SD of intracellular ion concentrations are always expressed as  $p_{ion}$  values, as only  $p_{ion}$  values were normally distributed (Fry et al.,

1990). Mean ion concentrations were then calculated from the mean pI<sub>on</sub> values.

## Iontophoretic injection

For iontophoretic injection of  $H^+$  and  $OH^-$ , conventional or theta-style glass microelectrodes (pulled from GC150–15 or TGC150F-15 glass capillaries; Clark, Reading, UK) were filled with 1 M HCl and/or 1 M KOH and connected to the current injection unit of an electrometer (Intra 767, WPI) via chlorided silver wires.  $H^+$  was injected into electrolyte droplets or living cells by passing a constant current of 1–5 nA through the HCl-filled barrel of the injection electrode, while  $OH^-$  was injected from the KOH-filled barrel by passing currents between –1 and –5 nA. For the iontophoretic injection of  $Mg^{2+}$ , conventional microelectrodes (GC150–15; Clark) were filled with 1 M  $MgCl_2$  and 20 mM MES to prevent the formation of  $Mg(OH)_2$  at the tip of the electrode, which was thought to be responsible for the observed clogging of the electrode in the absence of MES. Although this solution had a pH value of ~3.4, there seemed to be no significant co-injection of  $H^+$  during  $Mg^{2+}$  injection, as no pH changes were observed in neurons and ATP-free electrolyte droplets.

## Electrolyte droplets

Control experiments were carried out on electrolyte droplets containing an ionic background of (in mM) 110 KCl, 10 NaCl, 10 HEPES, pH 7.3 adjusted with KOH. In ATP-containing droplets, NaCl was replaced by nominally 5 mM  $Na_2ATP$  (Sigma, Deisenhofen, Germany). When investigating the pH dependence of  $Mg^{2+}$  binding to ATP, 5 mM  $MgCl_2$  was added to this ATP-containing solution.

$Na_2ATP$  is very hygroscopic, and it was attempted to estimate the amount of absorbed water from a comparison of the signals of a  $Na^+$ -sensitive microelectrode in a 10 mM  $Na^+$  calibration solution and a solution where 10 mM NaCl was replaced by nominally 5 mM  $Na_2ATP$ . From these measurements a purity of the  $Na_2ATP$  of ~95% was deduced; i.e., a nominal ATP concentration of 5 mM corresponded to an ATP content of 4.75 mM.

Three to five droplets with a diameter of 100–200  $\mu m$  (as determined by using a stereomicroscope with graded ocular lens; Leitz, Wetzlar, Germany) were squeezed from a broken glass capillary and placed on a grounded silver wire under paraffin oil (heavy white oil (Sigma) see Günzel et al., 1999). In addition, a reference droplet containing standard leech saline buffered to pH 7.4 with 50 mM HEPES was also placed on the wire. After the calibration of an ion-selective microelectrode, the tip of the electrode was inserted into this droplet and all electrode potentials were adjusted to 0 mV. The electrode could then be moved to one of the other droplets, as the ion-selective microelectrode, like the injection electrode, tolerated quick movements through the paraffin oil. After every successful experiment, the ion-selective microelectrode was moved back into the reference droplet to check for drift of the electrode signal.

Initially, some droplets were additionally stained with a pH-indicator dye (phenol red, Aldrich, Milwaukee, WI) to visualize the elicited pH changes and to ensure that pH in the reference droplet remained constant.

## Determination of cell volume changes

Retzius neurons were loaded with TMA (final  $[TMA]_i$  3–5 mM) by exposing them to a bath solution containing 5 mM TMA for 10–20 min. After removal of TMA from the bath solution  $[TMA]_i$  decreased slowly over a time course of 1–1.5 h. This decrease could be fitted by two exponential curves. As previously described (Dierkes et al., 2001), cell swelling leads to a proportional decrease in  $[TMA]_i$  below this curve and cell shrinkage to a proportional  $[TMA]_i$  increase.

## Determination of $[ATP]_i$ , $[ADP]_i$ , and $[AMP]_i$

To determine the total intracellular concentrations of ATP, ADP, and AMP ( $[ATP]_i$ ,  $[ADP]_i$ , and  $[AMP]_i$ ), Retzius neurons had to be isolated. To this end, whole ganglia were treated with collagenase/dispase for 70 min, after the ganglion sheath was disrupted with a fine glass knife. After several washes in standard leech saline the ganglion sheath was removed and the cell bodies of the Retzius neurons were isolated with a glass capillary, using gentle suction. The single cells were washed in a droplet of ice-cold standard leech saline and all the cells (5–12) isolated from one animal were pooled and frozen together in ~50  $\mu l$  of standard leech saline at –20°C until further use.

The protocol used for the determination of  $[ATP]_i$ ,  $[ADP]_i$ , and  $[AMP]_i$  was similar to that described by Strotmann et al. (1986). Each preparation was extracted by adding 400  $\mu l$  of boiling buffer solution containing 100 mM Tris and 4 mM EDTA (pH 7.75) and subsequent boiling for 2 min. Cell fragments were sedimented by centrifugation (1 min at 10,000  $\times g$ ). Three 100- $\mu l$  aliquots of the supernatant were incubated at room temperature for 1 h with 25  $\mu l$  of 1) an incubation medium containing (in mM) 17.5 HEPES, 37.5  $MgSO_4$ , 135 KCl, 1.05 phosphoenol pyruvate; 2) 25  $\mu l$  of incubation medium plus 2.5 U of pyruvate kinase to convert ADP into ATP; and 3) 25  $\mu l$  of incubation medium plus 2.5 U of pyruvate kinase (Boehringer, Mannheim, Germany) and 3.15 U of myokinase (Sigma) to convert ADP and AMP into ATP. To stop the reactions the samples were frozen and then thawed at 100°C.

A 50- $\mu l$  volume of each sample was mixed with 100  $\mu l$  of the monitoring reagent (LKB 1243–200), and bioluminescence was monitored with a luminometer (LKB 1250). The signals were calibrated by the addition of 50  $\mu l$  of 0.1 nM or 1 nM ATP.

## RESULTS

### pH dependence of $Mg^{2+}$ binding to ATP in electrolyte droplets

Initial experiments on electrolyte droplets stained with the pH indicator dye phenol red showed that diffusion of iontophoretically injected  $H^+$  and  $OH^-$  ions is a process that requires several seconds before a homogenous pH distribution within droplets of 100–200  $\mu m$  in diameter is reached. Thus, in experiments on the pH dependence of  $Mg^{2+}$  binding to ATP, pH and  $[Mg^{2+}]$  could not be measured with two separate microelectrodes but had to be measured within the same spot to be able to directly correlate the changes in these two parameters. This requirement could be fulfilled by the use of triple-barreled pH- and  $Mg^{2+}$ -sensitive microelectrodes. But even under these conditions it was not clear whether an error due to the different time constants of the pH-sensitive barrel and the  $Mg^{2+}$ -sensitive barrel would have to be expected. To be able to judge the size of such an error, pH was varied within an electrolyte droplet containing 5 mM ATP and 5 mM total  $Mg^{2+}$  by alternate injection of  $H^+$  and  $OH^-$ . For injection, a theta-style microelectrode was used, one barrel of which was filled with HCl, the other with KOH. The resulting changes in pH and in the free  $Mg^{2+}$  concentration within the droplet ( $pH_{dr}$  and  $[Mg^{2+}]_{dr}$ , respectively) were measured simultaneously with a  $Mg^{2+}$ /pH-sensitive microelectrode (inset in Fig. 1). A summary of six such experiments is shown in Fig. 1. In this figure,  $[Mg^{2+}]_{dr}$  values during acidification and alkalinization of

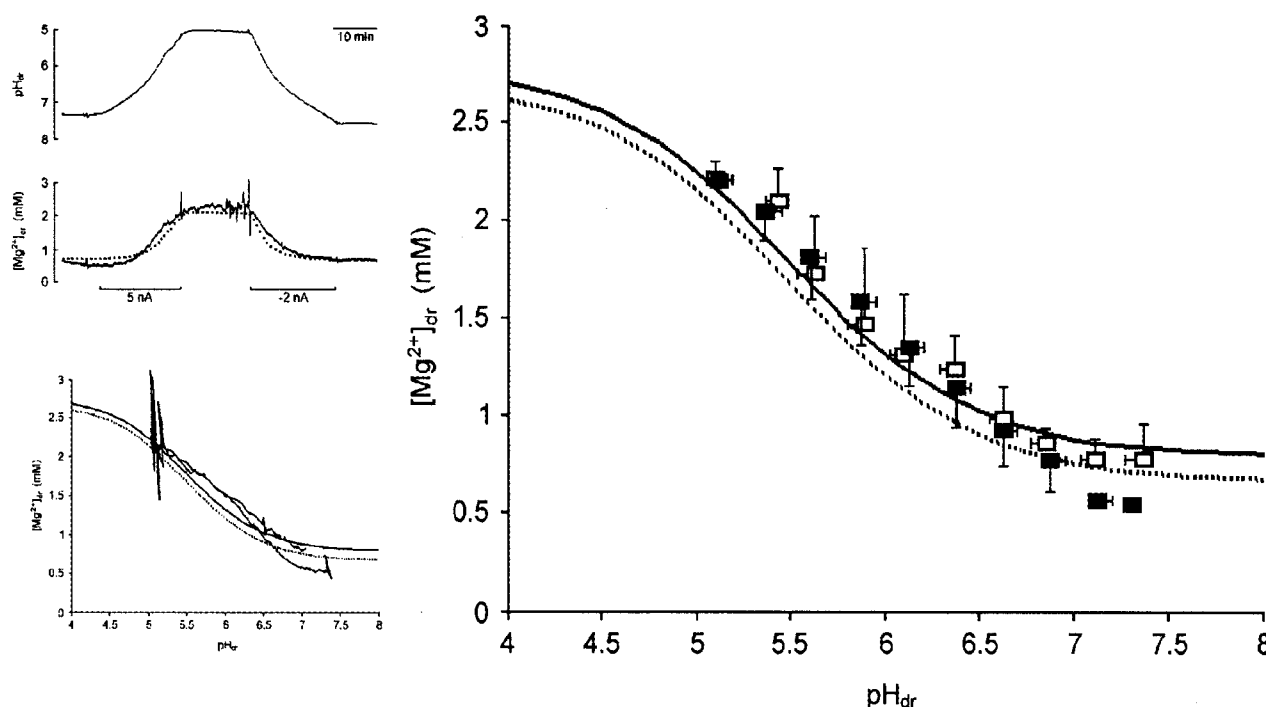


FIGURE 1 Relationship between pH and  $\text{Mg}^{2+}$  in an electrolyte droplet containing ATP. The dependence of the free  $\text{Mg}^{2+}$  concentration ( $[\text{Mg}^{2+}]_{\text{dr}}$ ) on the pH ( $\text{pH}_{\text{dr}}$ ) within an electrolyte droplet containing a total  $\text{Mg}^{2+}$  concentration and a total, nominal ATP concentration of 5 mM was measured during iontophoretic injection of  $\text{H}^+$  and  $\text{OH}^-$ . The  $[\text{Mg}^{2+}]_{\text{dr}}$  values during acidification (■) and alkalinization (□) of the droplets were grouped in classes of 0.25 pH units, averaged, and plotted against the mean  $\text{pH}_{\text{dr}}$  within each class. The curves are the relationships between pH and  $\text{Mg}^{2+}$  calculated from Eq. 2 (Appendix), assuming an ATP purity of 100% (dotted line) and 95% (solid line) and the pH dependence of the apparent dissociation constant ( $K_{\text{ATP}}$ ) for  $\text{Mg}^{2+}$  binding to ATP determined by Lüthi et al. (1999) (Appendix, Eq. 4). (Inset) Original recording of  $[\text{Mg}^{2+}]_{\text{dr}}$  and  $\text{pH}_{\text{dr}}$  during iontophoretic injection of  $\text{H}^+$  and  $\text{OH}^-$  into an electrolyte droplet and plot of the  $[\text{Mg}^{2+}]_{\text{dr}}$  versus the  $\text{pH}_{\text{dr}}$  values obtained during this experiment. Lines were calculated for 100% (dotted) and 95% (solid) ATP purity, respectively.

the droplets were grouped in classes of 0.25 pH units, averaged, and plotted against the mean  $\text{pH}_{\text{dr}}$  within each class. As there was no significant difference between  $[\text{Mg}^{2+}]_{\text{dr}}$  values during acidification and alkalinization it was concluded that differences in the response time of the two barrels of the ion-selective microelectrode did not affect the accuracy of the measurements. The measured values were in reasonable agreement with the pH dependence of  $\text{Mg}^{2+}$  binding to ATP (dotted line in Fig. 1) calculated from the recently determined apparent equilibrium constant ( $K_{\text{ATP}}$ , Lüthi et al., 1999), especially if it was taken into account that the  $\text{Na}_2\text{ATP}$  used had absorbed water so that the solutions contained only  $\sim 95\%$  of the intended 5 mM (solid line in Fig. 1; see Materials and Methods).

### pH dependence of $[\text{Mg}^{2+}]_{\text{i}}$ in Retzius neurons

In Retzius neurons,  $\text{H}^+$  and  $\text{OH}^-$  were injected from separate, conventional glass microelectrodes, while  $\text{pH}_{\text{i}}$ ,  $[\text{Mg}^{2+}]_{\text{i}}$  and  $E_{\text{m}}$  were measured simultaneously with a triple-barreled  $\text{Mg}^{2+}$ /pH-sensitive microelectrode. While an injection of  $\text{OH}^-$  did not affect  $[\text{Mg}^{2+}]_{\text{i}}$  in Retzius neurons (Günzel et al., 1999), an acidification via  $\text{H}^+$  injection

caused an increase in  $[\text{Mg}^{2+}]_{\text{i}}$  (Fig. 2 A). Because of the positive injection current, the neurons depolarized substantially. After termination of the  $\text{H}^+$  injection, both  $E_{\text{m}}$  and  $\text{pH}_{\text{i}}$  recovered within  $\sim 20$  min through cell-inherent processes (see below), so that, in contrast to the experiments on electrolyte droplets, no  $\text{OH}^-$  injection was required. pH recovery was accompanied by a further, transient increase in  $[\text{Mg}^{2+}]_{\text{i}}$ . A plot of  $[\text{Mg}^{2+}]_{\text{i}}$  against  $\text{pH}_{\text{i}}$  (Fig. 2 B) therefore resulted in a loop. The ascending branch of these loops could be fitted using Eqs. 2 and 4 (Appendix), assuming an average  $[\text{ATP}]_{\text{i}}$  of  $3.1 \pm 1.1$  mM and an average  $[\text{Mg}]_{\text{i}}$  of  $3.1 \pm 1.4$  mM ( $n = 6$ ).

To determine whether the transient  $[\text{Mg}^{2+}]_{\text{i}}$  increase during pH recovery of the neuron was due to an influx of  $\text{Mg}^{2+}$ ,  $\text{H}^+$  injections were carried out in neurons which were exposed to a nominally  $\text{Mg}^{2+}$  free bath solution (Fig. 3A). During such an exposure,  $[\text{Mg}^{2+}]_{\text{i}}$  of the neurons gradually decreased. The injection of  $\text{H}^+$  again caused an increase in  $[\text{Mg}^{2+}]_{\text{i}}$ . However, the transient increase in  $[\text{Mg}^{2+}]_{\text{i}}$  after termination of the injection was completely absent. Thus, in the plot of  $[\text{Mg}^{2+}]_{\text{i}}$  against  $\text{pH}_{\text{i}}$  (Fig. 3B) the ascending and the descending branch are superimposed. Again, the pH dependence of  $[\text{Mg}^{2+}]_{\text{i}}$  could be fitted with



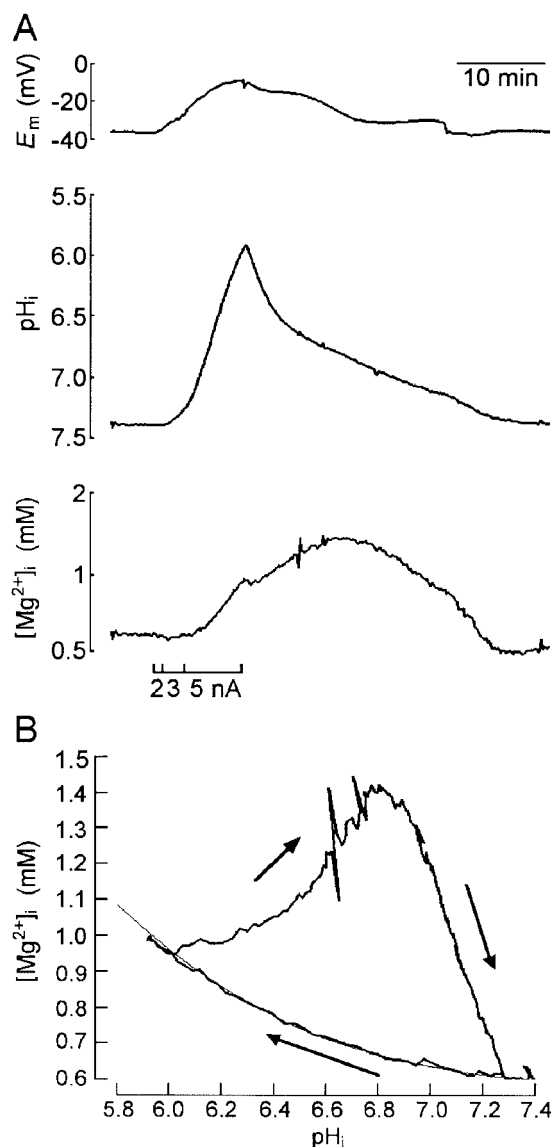


FIGURE 2 Relationship between pH and  $Mg^{2+}$  in a Retzius neuron in the presence of extracellular  $Mg^{2+}$ . (A) Original recording of the intracellular free  $Mg^{2+}$  concentration ( $[Mg^{2+}]_i$ ), the intracellular pH ( $pH_i$ ), and the membrane potential ( $E_m$ ) of a Retzius neuron exposed to standard leech saline. The neuron was acidified through iontophoretic injection of  $H^+$  (using currents between 2 and 5 nA). (B)  $[Mg^{2+}]_i$  values from the experiment shown in A were plotted against the corresponding  $pH_i$  values. During acidification the relationship could be fitted by a curve calculated for a total ATP concentration of 3 mM and a total  $Mg^{2+}$  concentration of 3.1 mM (Eqs. 2 and 4, Appendix). During re-alkalinization there was a further increase in  $[Mg^{2+}]_i$ , which cannot be explained by  $Mg^{2+}$  binding to ATP.

Eqs. 2 and 4 (Appendix), assuming an average  $[ATP]_i$  of  $2.8 \pm 0.9$  mM and an average  $[Mg]_i$  of  $1.8 \pm 0.7$  mM ( $n = 4$ ). The low value for  $[Mg]_i$  reflects the net loss of  $Mg^{2+}$  from the cells during exposure to  $Mg^{2+}$  free saline, while  $[ATP]_i$  was not influenced by the experimental conditions and ranged between 2 and 4 mM in the presence and nominal absence of  $[Mg^{2+}]_o$ .

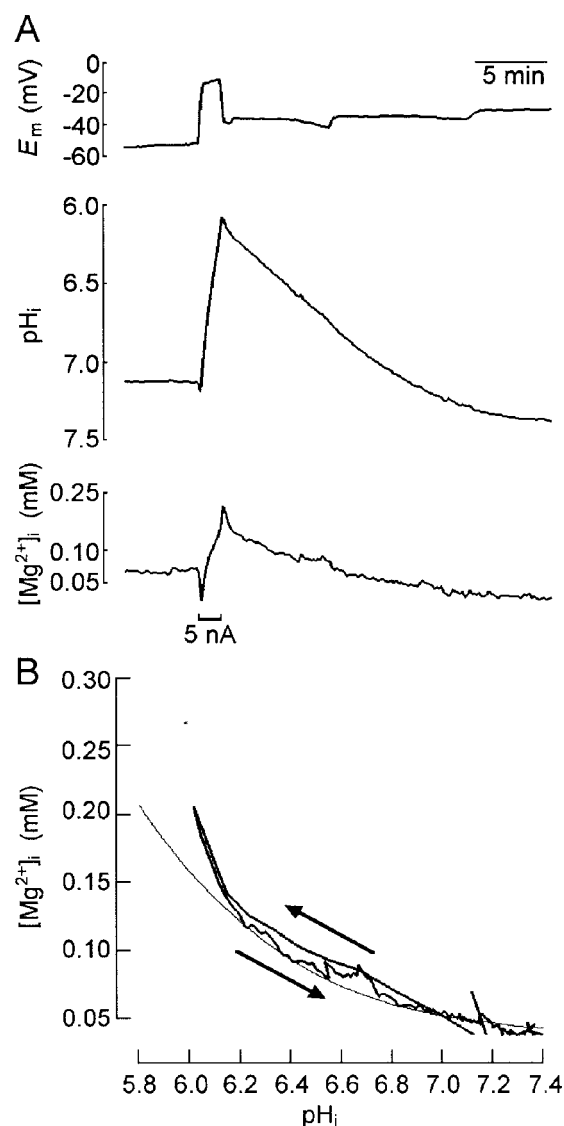


FIGURE 3 Relationship between pH and  $Mg^{2+}$  in a Retzius neuron in the nominal absence of extracellular  $Mg^{2+}$ . (A) Original recording of the intracellular free  $Mg^{2+}$  concentration ( $[Mg^{2+}]_i$ ), the intracellular pH ( $pH_i$ ), and the membrane potential ( $E_m$ ) of a Retzius neuron exposed to nominally  $Mg^{2+}$ -free saline. The neuron was acidified through iontophoretic injection of  $H^+$  (using a current of 5 nA). (B)  $[Mg^{2+}]_i$  values from the experiment shown in A were plotted against the corresponding  $pH_i$  values. In contrast to the experiment shown in Fig. 2, the relationship could be fitted by a curve calculated for a total ATP concentration of 3 mM and a total  $Mg^{2+}$  concentration of 1.1 mM (Eqs. 2 and 4, Appendix) during both acidification and re-alkalinization.

### Intracellular concentration of adenosine phosphates in Retzius neurons

Initial determinations of  $[ATP]_i$  in Retzius neurons using the luciferin/luciferase bioluminescence assay yielded values of  $17.7 \pm 8.8$  fmol/cell ( $n = 25$  cells from four animals, equivalent to  $<0.1$  mM; see below), indicating that most of the ATP had degraded during the preparation procedure.

Although incubation of the preparations in solutions containing 0.1 mM ouabain to block  $\text{Na}^+/\text{K}^+$ -ATPase activity increased  $[\text{ATP}]_i$  values significantly to  $199.1 \pm 66.5$  fmol/cell ( $n = 50$  cells from six animals) these values were still considered unphysiologically low. Therefore,  $[\text{ADP}]_i$  and  $[\text{AMP}]_i$  were determined in the same samples. The mean  $[\text{ADP}]_i$  was found to be  $1723 \pm 424$  fmol/cell, the mean  $[\text{AMP}]_i$   $79.8 \pm 613$  fmol/cell. Thus, most of the ATP seemed to have degraded to ADP whereas a further degradation to AMP was negligible.

Cell diameters of Retzius neurons were determined using a stereomicroscope with a graded ocular lens and found to be  $83.2 \pm 6.5$   $\mu\text{m}$  ( $n = 14$  cells from three animals). From these values it was calculated that the sum of the total intracellular  $[\text{ADP}]_i$  and  $[\text{ATP}]_i$  was  $5.9 \pm 1.5$  mM ( $n = 6$ ). Assuming that under physiological conditions  $[\text{ATP}]_i$  in neurons makes up 80–90% of this value (Pissarek et al. 1998; Plaschke et al. 1998), the estimate of  $[\text{ATP}]_i$  in Retzius neurons would be in the range of 4.6 to 5.1 mM, which, considering the inaccuracies of the two methods, is in good agreement with the values estimated from the  $\text{H}^+$ -injection experiments.

### Effects of $\text{H}^+$ injections on $[\text{Na}^+]_i$ , $[\text{K}^+]_i$ , and the cell volume

In the nominal absence of  $\text{HCO}_3^-$ ,  $\text{pH}_i$  recovery after an acidification in Retzius neurons is known to be due to a  $\text{Na}^+/\text{H}^+$  antiport (Schlue and Thomas, 1985). This might lead to an increase in  $[\text{Na}^+]_i$ , which could be large enough to shift the equilibrium of the  $\text{Na}^+/\text{Mg}^{2+}$  antiport and thus cause the transient  $[\text{Mg}^{2+}]_i$  increase. Therefore,  $\text{H}^+$  was injected into Retzius neurons in the presence and in the absence of extracellular  $\text{Mg}^{2+}$ , whereas  $[\text{Na}^+]_i$  and  $\text{pH}_i$  were recorded with a  $\text{Na}^+/\text{pH}$ -sensitive microelectrode. As shown in Fig. 4 A,  $[\text{Na}^+]_i$  increased considerably. In seven such experiments a mean  $[\text{Na}^+]_i$  value of  $41.1$  mM ( $\text{pNa} = 1.39 \pm 0.08$ ) was obtained during  $\text{H}^+$  injections to a mean  $\text{pH}_i$  of  $5.66 \pm 0.14$ .  $[\text{Na}^+]_i$  remained high during the initial phase of  $\text{pH}_i$  recovery and then decreased toward its initial value. As in the case of  $[\text{Mg}^{2+}]_i$ , a plot of  $[\text{Na}^+]_i$  against  $\text{pH}_i$  resulted in a loop. The shape of this loop was independent of the extracellular  $\text{Mg}^{2+}$  concentration ( $[\text{Mg}^{2+}]_o$ , Fig. 4 B).

The increases in  $[\text{Na}^+]_i$  were paralleled by decreases in the intracellular  $\text{K}^+$  concentration ( $[\text{K}^+]_i$ ) from a mean value of  $74.3$  mM ( $\text{pK} 1.13 \pm 0.02$ ,  $n = 4$ ) to a mean of  $36.5$  mM ( $\text{pK} 1.44 \pm 0.06$ ,  $n = 4$ , during intracellular acidification to a mean  $\text{pH}_i$  of  $5.73 \pm 0.06$ ,  $n = 4$ , not shown). During the duration of six additional  $\text{H}^+$  injections (to a mean  $\text{pH}_i$  of  $5.56 \pm 0.1$ , not shown), there was no significant change in cell volume ( $4.2 \pm 5.9\%$ ,  $n = 6$ , as measured with TMA-sensitive microelectrodes in TMA-loaded neurons). The cell swelling of  $10.7 \pm 4.7\%$  ( $n = 6$ ) that was observed during the re-alkalinization of these neurons was

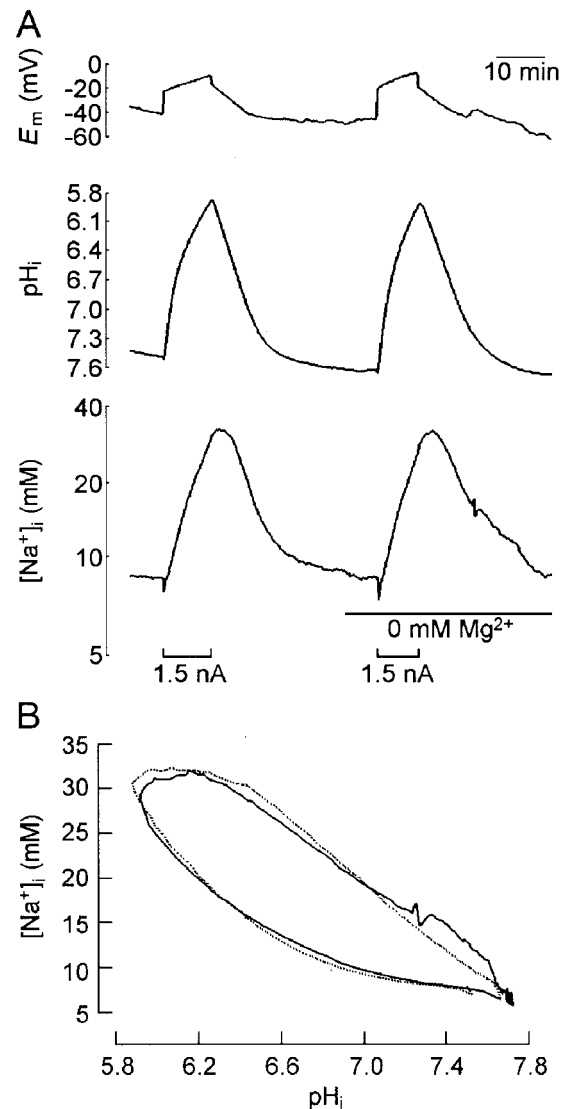


FIGURE 4 Relationship between pH and  $\text{Na}^+$  in a Retzius neuron in the presence and in the nominal absence of extracellular  $\text{Mg}^{2+}$ . (A) Original recording of the intracellular  $\text{Na}^+$  concentration ( $[\text{Na}^+]_i$ ), the intracellular pH ( $\text{pH}_i$ ), and the membrane potential ( $E_m$ ) of a Retzius neuron exposed to standard leech saline and nominally  $\text{Mg}^{2+}$ -free saline. The neuron was acidified through iontophoretic injection of  $\text{H}^+$  (using a current of 1.5 nA). After acidification,  $[\text{Na}^+]_i$  increased substantially. This increase was similar in the presence and nominal absence of  $\text{Mg}^{2+}$  and was attributed to the activation of the  $\text{Na}^+/\text{H}^+$  antiport. (B)  $[\text{Na}^+]_i$  values from the experiment shown in A were plotted against the corresponding  $\text{pH}_i$  values. The observed relationships were independent of the extracellular  $\text{Mg}^{2+}$  concentration (dotted line, 1 mM  $\text{Mg}^{2+}$ ; solid line, nominally  $\text{Mg}^{2+}$ -free).

moderate as the large increase in  $[\text{Na}^+]_i$  was counteracted by the parallel decrease in  $[\text{K}^+]_i$ .

### Effect of the application of ouabain on $[\text{Na}^+]_i$ , $[\text{Mg}^{2+}]_i$ , and $\text{pH}_i$

To gain further proof that the increase in  $[\text{Na}^+]_i$  was the cause of the additional increase in  $[\text{Mg}^{2+}]_i$ , an increase in

$[\text{Na}^+]_i$  was elicited through inhibition of the  $\text{Na}^+/\text{K}^+$  pump by the application of ouabain. Initial experiments that were carried out with 1 mM ouabain in standard leech saline resulted in huge increases in  $[\text{Na}^+]_i$  to a mean value of 111.8 mM ( $p\text{Na} = 0.95 \pm 0.04$ ,  $n = 6$ ), a mean increase in  $[\text{Mg}^{2+}]_i$  of 0.3 mM ( $\Delta p\text{Mg} = -0.31 \pm 0.17$ ,  $n = 11$ ), and a mean decrease in pH of  $0.3 \pm 0.16$  pH units ( $n = 5$ ). To reduce  $[\text{Na}^+]_i$  increases to values more comparable to those observed after  $\text{H}^+$  injections, the ouabain concentration was reduced to 0.5 mM and the extracellular  $\text{Na}^+$  concentration to 45 mM by equimolar substitution with NMDG $^+$ . Under these conditions, an increase in  $[\text{Na}^+]_i$  to a mean concentration of 31.4 mM ( $p\text{Na} = 1.50 \pm 0.28$ ,  $n = 4$ ), a mean increase in  $[\text{Mg}^{2+}]_i$  of 0.14 mM ( $\Delta p\text{Mg} = -0.27 \pm 0.25$ ,  $n = 4$ ), and a mean decrease in pH of  $0.15 \pm 0.03$  pH units ( $n = 3$ ) were observed.

### Injection of $\text{Mg}^{2+}$ into ATP-free and ATP-containing electrolyte droplets

To investigate intracellular  $\text{Mg}^{2+}$  muffling,  $\text{Mg}^{2+}$  was iontophoretically injected into Retzius neurons. To be able to estimate the quantity of the injected  $\text{Mg}^{2+}$ , the transport index (TI) for  $\text{Mg}^{2+}$  in a  $\text{MgCl}_2$  solution had to be determined. In theory, TI can be calculated from the ion motility and would amount to  $\sim 0.41$  (Atkins, 1994); i.e., 41% of the injection current should be carried by  $\text{Mg}^{2+}$  ions. As, however, TI has been reported to be dependent on the experimental conditions and on the microelectrodes used (Belan et al., 1993; Schwiening and Thomas, 1996), it was attempted to estimate TI under conditions similar to an intracellular

milieu. To this end,  $\text{Mg}^{2+}$  was iontophoretically injected into ATP-free and ATP-containing electrolyte droplets, using microelectrodes filled with  $\text{MgCl}_2$ , whereas  $[\text{Mg}^{2+}]_{\text{dr}}$  was measured with a  $\text{Mg}^{2+}$ -sensitive microelectrode.

A typical recording of a  $\text{Mg}^{2+}$  injection into an ATP-free electrolyte droplet is shown in Fig. 5 A. The increases in  $[\text{Mg}^{2+}]_i$  could be fitted if it was assumed that 38% of the current was carried by  $\text{Mg}^{2+}$ . From 11 such experiments a mean TI of  $0.34 \pm 0.098$  was obtained.

In another set of experiments,  $\text{Mg}^{2+}$  was injected into an electrolyte droplet containing nominally 5 mM ATP. In these experiments,  $\text{pH}_{\text{dr}}$  decreased continuously, as  $\text{H}^+$  was released from ATP with increasing  $[\text{Mg}^{2+}]_{\text{dr}}$ . Therefore,  $\text{pH}_{\text{dr}}$  was monitored in addition to  $[\text{Mg}^{2+}]_{\text{dr}}$ . The recordings, an example of which is shown in Fig. 5 B, were fitted using Eq. 2 (Appendix), taking into account the pH dependence of  $K_{\text{ATP}}$  found by Lüthi et al. (1999; Eq. 4, Appendix) and the estimated purity of ATP of 95% (see Materials and Methods and Fig. 1). Under these conditions, a mean TI of  $0.36 \pm 0.092$  had to be assumed to obtain optimal fits in 12 such experiments. This TI value was not significantly different from the TI value of 0.34 obtained in ATP-free electrolyte droplets, so that for further calculations the mean of all TI values,  $0.35 (\pm 0.093)$ ,  $n = 23$ , was used.

### Injection of $\text{Mg}^{2+}$ into Retzius neurons

$\text{Mg}^{2+}$  was injected into Retzius neurons either by passing a continuous current of  $\sim 5$  nA or with a series of short (1-s) pulses of  $\sim 25$  nA (Fig. 6 A). Using the TI value of 0.35 derived from the experiments on electrolyte droplets, the

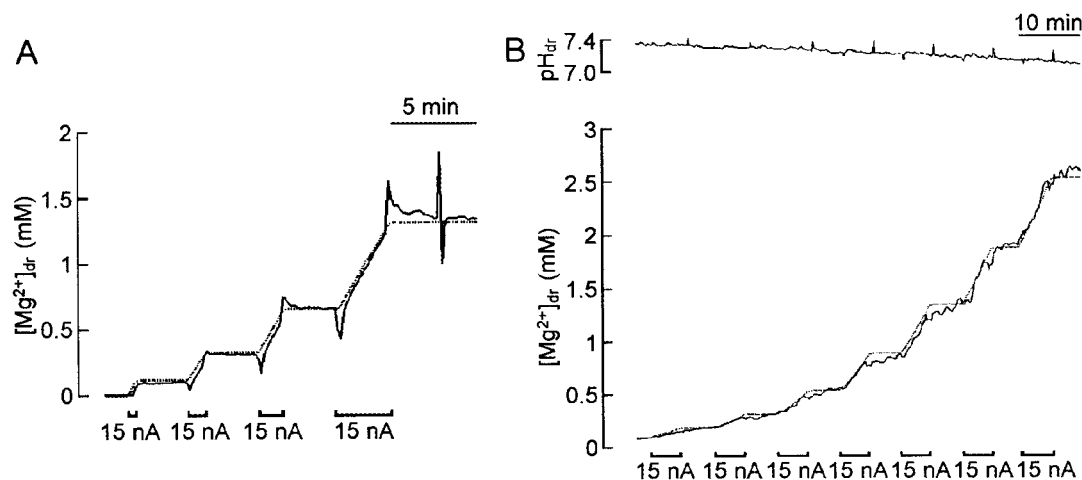


FIGURE 5 Iontophoretic injection of  $\text{Mg}^{2+}$  into an ATP-free and an ATP-containing electrolyte droplet. (A) Original recording of an iontophoretic injection of  $\text{Mg}^{2+}$  into an ATP-free electrolyte droplet. The observed increases in the free  $\text{Mg}^{2+}$  concentration ( $[\text{Mg}^{2+}]_{\text{dr}}$ ) corresponded well to the expected increases (dotted line) calculated from Eq. 1 (Appendix) if a transport index (TI) value of 0.38 was assumed. (B) Simultaneous recording of the free  $\text{Mg}^{2+}$  concentration ( $[\text{Mg}^{2+}]_{\text{dr}}$ ) and the pH ( $\text{pH}_{\text{dr}}$ ) during an iontophoretic injection of  $\text{Mg}^{2+}$  into an electrolyte droplet containing 5 mM ATP. The observed increases in the free  $\text{Mg}^{2+}$  concentration ( $[\text{Mg}^{2+}]_{\text{dr}}$ ) corresponded well to the expected increases (dotted line) calculated from Eqs. 1, 2, and 4 (Appendix), assuming a TI value of 0.34 mM.

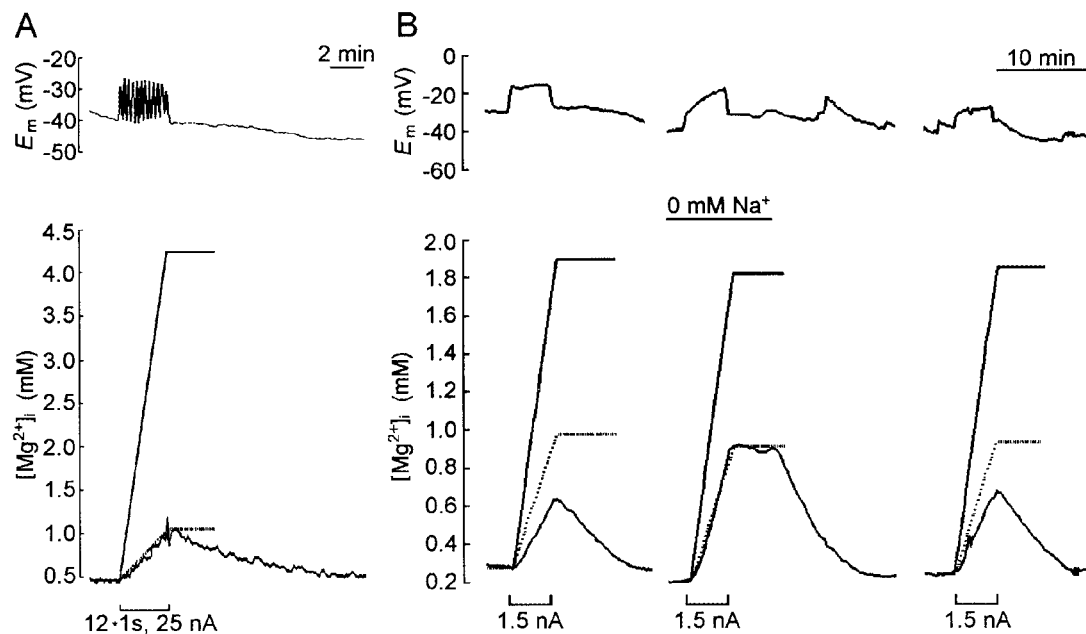


FIGURE 6 Iontophoretic injection of  $\text{Mg}^{2+}$  into a Retzius neuron in the presence and in the nominal absence of extracellular  $\text{Na}^+$ . (A) Original recording of an iontophoretic injection (12 pulses of 25 nA and a duration of 1 s) of  $\text{Mg}^{2+}$  into a Retzius neuron exposed to standard leech saline. The observed increases in the intracellular free  $\text{Mg}^{2+}$  concentration ( $[\text{Mg}^{2+}]_i$ ) were compared with the increase that would be expected (Eq. 1, Appendix;  $\text{TI} = 0.35$ ) if  $\text{Mg}^{2+}$  were not buffered (solid line) and assuming that 85.5% of the injected  $\text{Mg}^{2+}$  were buffered (dotted line, corresponding to a  $B_{\Delta\text{Mg}}$  value of 6.9). (B) Original recording of an iontophoretic injection (continuous current of 1.5 nA) of  $\text{Mg}^{2+}$  into a Retzius neuron exposed to  $\text{Na}^+$ -containing and to nominally  $\text{Na}^+$ -free saline. The observed increases in  $[\text{Mg}^{2+}]_i$  were considerably larger when the  $\text{Na}^+/\text{Mg}^{2+}$  antiport was blocked in the nominal absence of extracellular  $\text{Na}^+$ . The dotted lines were calculated from Eq. 1 (Appendix;  $\text{TI} = 0.35$ ) and under the assumption that 57% of the injected  $\text{Mg}^{2+}$  was buffered (corresponding to a  $B_{\Delta\text{Mg}}$  value of 2.33). To fit the increases obtained in the presence of extracellular  $\text{Na}^+$ ,  $B_{\Delta\text{Mg}}$  would have to be increased to 4. Solid line, expected increase in the absence of intracellular  $\text{Mg}^{2+}$  buffering.

increases in  $[\text{Mg}]_i$  ( $\Delta[\text{Mg}]_i$ ) could be calculated from Eq. 1 (Appendix). In 21 such experiments the mean  $\Delta[\text{Mg}]_i$  amounted to  $2.43 \pm 1.15$  mM. These increases in  $[\text{Mg}]_i$  resulted in an increase in  $[\text{Mg}^{2+}]_i$  from a mean initial value of 0.32 mM (pMg  $3.50 \pm 0.33$ ,  $n = 21$ ) to a mean  $[\text{Mg}^{2+}]_i$  of 0.70 mM (pMg  $3.15 \pm 0.32$ ,  $n = 21$ ), i.e., in a  $\Delta[\text{Mg}]_i$  of 0.38 mM. From the ratios of the individual  $\Delta[\text{Mg}]_i$  values and the resulting  $\Delta[\text{Mg}]_i$  values of these experiments, the mean muffling ratio  $B_{\Delta\text{Mg}} = \Delta[\text{Mg}]_i/\Delta[\text{Mg}^{2+}]_i$  was determined as  $7.57 \pm 5.23$  ( $n = 21$ ).

However, this ratio is not only influenced by  $\text{Mg}^{2+}$  bound or sequestered intracellularly but also by the amount of  $\text{Mg}^{2+}$  extruded from the cell, mainly via  $\text{Na}^+/\text{Mg}^{2+}$  antiport (Günzel and Schlue, 1996). To estimate the contribution of  $\text{Mg}^{2+}$  extrusion to  $\text{Mg}^{2+}$  muffling,  $\text{Mg}^{2+}$  extrusion was blocked by superfusing the preparation with a nominally  $\text{Na}^+$ -free saline. When  $\text{Mg}^{2+}$  was injected under these conditions, the resultant increase in  $[\text{Mg}^{2+}]_i$  was significantly larger than in the presence of extracellular  $\text{Na}^+$  (Fig. 6 B), causing a decrease in  $B_{\Delta\text{Mg}}$  to  $4.4 \pm 1.71$  ( $n = 7$ ). Due to the inhibition of the  $\text{Na}^+/\text{Mg}^{2+}$  antiport  $[\text{Mg}^{2+}]_i$  remained increased (plateau in Fig. 6 B) until  $\text{Na}^+$  was again added to the bath solution.

## DISCUSSION

### Iontophoretic injection of $\text{H}^+$ and $\text{Mg}^{2+}$ into Retzius neurons

Comparison of experiments carried out in electrolyte droplets and neurons showed that iontophoretic ion injection was a reliable method for studying intracellular  $\text{Mg}^{2+}$  muffling. A problem inherent to iontophoretic injection of cations is, however, that depolarizing currents must be used. Due to the substantial depolarization during  $\text{H}^+$  and  $\text{Mg}^{2+}$  injections (Figs. 2–4),  $\text{Ca}^{2+}$  is expected to enter the cells, and this might influence intracellular  $\text{Mg}^{2+}$  buffering through competition at the binding sites (Kato et al., 1998). In Retzius neurons, however, such effects did not appear to play an essential role. First, depolarizations elicited by the application of high extracellular  $\text{K}^+$  concentrations did not cause any increase in  $[\text{Mg}^{2+}]_i$  (Müller et al., 1997). Second, there was no difference in  $\text{Mg}^{2+}$  muffling between experiments in which a continuous injection current was used and those in which  $\text{Mg}^{2+}$  was injected in a sequence of short pulses (compare Fig. 6, A and B).

An additional potential source of artifacts was that volume changes might have been caused by the changes in



$[\text{Na}^+]_i$  and  $[\text{K}^+]_i$  after  $\text{H}^+$  injection. Determination of volume changes during and after  $\text{H}^+$  injection showed that there was indeed significant cell swelling several minutes after  $\text{H}^+$  injection, which might have led to an underestimation of the increase in  $[\text{Mg}^{2+}]_i$  during the re-alkalinization of the neurons (see Fig. 2). During  $\text{H}^+$  injection, the part of the relationship between pH and  $[\text{Mg}^{2+}]_i$  used for the estimation of the intracellular ATP concentration, however, was not significantly affected by volume changes.

### Evaluation of intracellular $\text{Mg}^{2+}$ muffling

A wide variety of definitions has been used to express the amount of intracellular buffering/muffling, mainly for  $\text{H}^+$  and  $\text{Ca}^{2+}$  but also for  $\text{Mg}^{2+}$  (for review see Neher, 1995; Lüthi et al., 1999). While  $\text{H}^+$  and  $\text{Ca}^{2+}$  buffering usually is defined on a logarithmic scale, e.g., the change in the total ion concentration per unit of  $\text{p}(\text{ion})$  ( $\text{p}(\text{ion}) = -\log[\text{ion}]$ ),  $\text{Mg}^{2+}$  buffering generally is expressed on a linear scale. This is probably due to the fact that changes in  $[\text{Mg}^{2+}]_i$  are small, whereas the intracellular free concentration of  $\text{H}^+$  and  $\text{Ca}^{2+}$  may change over one order of magnitude or more.

The definition used for  $\text{Mg}^{2+}$  buffering/muffling by different authors depends on their experimental design. A direct determination of the concentration and dissociation constants of intracellular buffers is possible only in systems in which intracellular sequestration and transport across cell membranes can be ruled out. This is the case in studies on permeabilized erythrocytes (Flatman and Lew, 1980; Flatman, 1988) or cells (Günther et al., 1995). In these studies it was concluded that mammalian erythrocytes possess at least two different non-ATP  $\text{Mg}^{2+}$  buffer systems. One of these buffers is 2,3-bisphosphoglycerate (Flatman and Lew, 1980; Flatman, 1988; Günther et al., 1995); the other is believed to consist of hemoglobin (Raftos et al., 1999). These are the only experiments that directly determine  $\text{Mg}^{2+}$  buffering rather than  $\text{Mg}^{2+}$  muffling.

An alternative experimental approach is the induction of small  $[\text{Mg}^{2+}]_i$  increases in intact cells, e.g., by  $\text{Mg}^{2+}$  injection. In these studies,  $\text{Mg}^{2+}$  muffling is usually expressed by relating the changes in  $[\text{Mg}^{2+}]_i$  ( $\Delta[\text{Mg}^{2+}]_i$ ) to the changes in  $[\text{Mg}]_t$  ( $\Delta[\text{Mg}]_t$ ). Thus, Csernoch et al. (1998) and Westerblad and Allen (1992) use the ratio  $\Delta[\text{Mg}^{2+}]_i/\Delta[\text{Mg}]_t$ . The reciprocal of this ratio, the muffling ratio  $\Delta[\text{ion}]_t/\Delta[\text{ion}]_i$ , is used by Schwiening and Thomas (1996) in their study on  $\text{Ca}^{2+}$  muffling. A similar expression is introduced by Koss et al. (1993), who define the buffer coefficient  $B_{\text{Mg}}$  as  $d[\text{Mg}]_t/d\alpha[\text{Mg}^{2+}]_i$  ( $\alpha$  being the activity coefficient). In their further calculations, however, they actually use  $\Delta[\text{Mg}]_t/\Delta\alpha[\text{Mg}^{2+}]_i$ . This ratio will be abbreviated as  $B_{\Delta\text{Mg}}$  within the present discussion (irrespective of whether it is defined in terms of ion activities, as by Koss et al. (1993), or in terms of ion concentrations, as by Schwiening and Thomas (1996)). According to Koss et al. (1993),  $B_{\Delta\text{Mg}}$  is "a unitless indicator expressing the millimolar

amount of  $\text{Mg}^{2+}$  that must be added to raise cytosolic  $\alpha\text{Mg}^{2+}$  by 1 mM." This, however, is incorrect, as  $B_{\Delta\text{Mg}}$  itself depends both on the initial value of  $[\text{Mg}^{2+}]_i$  and on the amount of  $\text{Mg}^{2+}$  added ( $\Delta[\text{Mg}]_t$ ) as demonstrated in Fig. 7 A (see also Eqs. 5–7).  $B_{\Delta\text{Mg}}$  approaches a constant value only for infinitesimal or for very large values of  $\Delta[\text{Mg}]_t$  and  $[\text{Mg}^{2+}]_i$ . At physiological  $[\text{Mg}^{2+}]_i$  and under most experimental conditions  $B_{\Delta\text{Mg}}$  varies widely (shaded area in Fig. 7 A). This makes a comparison of  $B_{\Delta\text{Mg}}$  values from different studies almost impossible and even a comparison within the same preparation very difficult.

A possibility to describe  $\text{Mg}^{2+}$  muffling independently of experimental conditions is to express it in terms of a total

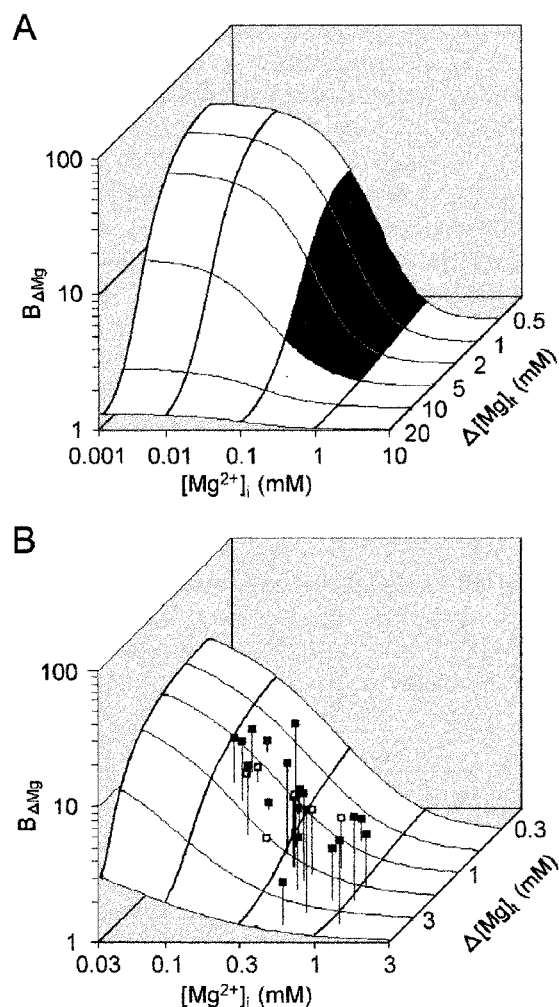


FIGURE 7 Dependence of  $B_{\Delta\text{Mg}}$  on  $[\text{Mg}^{2+}]_i$  and  $\Delta[\text{Mg}]_t$ . (A) Dependence of  $B_{\Delta\text{Mg}}$  on  $[\text{Mg}^{2+}]_i$  and  $\Delta[\text{Mg}]_t$ , calculated from Eqs. 2 and 5 (Appendix) for an  $[\text{ATP}]_t$  of 5 mM and a  $K_{\text{ATP}}$  of 0.117 mM. The black area denotes the range of values from the present study and illustrates that  $B_{\Delta\text{Mg}}$  has to be expected to vary over a wide range. (B) Enlarged view from A.  $B_{\Delta\text{Mg}}$  values obtained from experiments carried out in the presence (■) and nominal absence (□) of extracellular  $\text{Na}^+$  all lie above the calculated area, indicating that there have to be additional buffering/muffling systems besides ATP and  $\text{Mg}^{2+}$  extrusion via the  $\text{Na}^+/\text{Mg}^{2+}$  antiporter. Vertical lines represent the projections onto the theoretical relationship.

concentration ( $[\text{Bu}]_i$ ) and apparent dissociation constant ( $K_{\text{Bu}}$ ) of a buffer equivalent to the amount of muffling observed. In contrast to  $B_{\Delta\text{Mg}}$ ,  $[\text{Bu}]_i$  and  $K_{\text{Bu}}$  are independent of the initial  $[\text{Mg}^{2+}]_i$  and the amount of  $\text{Mg}^{2+}$  added and thus make it easier to compare values found in various studies. In the absence of intracellular sequestration and membrane transport this approach is identical to the first one discussed above, whereas in their presence these processes will contribute to the values of  $[\text{Bu}]_i$  and  $K_{\text{Bu}}$ . If one or several components of intracellular muffling are already known (e.g., the intracellular ATP concentration) or can be inhibited (e.g., transport across the cell membrane), their contribution to the intracellular muffling can be treated separately (see Eqs. 3 and 7). One of the advantages of the use of a buffer equivalent to express intracellular muffling is that it allows comparison of the results from studies with very different experimental designs. Thus, an estimate of the concentration and the affinity of a non-ATP buffer equivalent is possible from the data of Westerblad and Allen (1992), Koss et al. (1993), and Koss and Grubbs (1994).  $[\text{Bu}]_i$  calculated from these publications amount to 18.7, 12, and 8.5 mM, respectively. The respective values for  $K_{\text{Bu}}$  are 0.7, 1.3, and 1 mM. While Koss et al. (1993) and Koss and Grubbs (1994) exclude  $\text{Mg}^{2+}$  muffling due to extrusion during their experiments it seems likely that the comparatively high value for  $[\text{Bu}]_i$  calculated from Westerblad and Allen (1992) reflects the contribution of  $\text{Mg}^{2+}$  extrusion from the cells during the course of these experiments.

Irrespective of an expression of  $\text{Mg}^{2+}$  buffering as  $B_{\Delta\text{Mg}}$  or as a buffer equivalent it has to be kept in mind that the obtained values will always depend on the speed of the induced change in  $[\text{Mg}^{2+}]_i$ . For very fast changes in  $[\text{Mg}^{2+}]_i$  it has to be expected that  $B_{\Delta\text{Mg}}$  decreases and  $[\text{Bu}]_i$  approaches a value truly equivalent to cytosolic buffering (i.e., without any contribution of extrusion and sequestration), whereas for very slow changes in  $[\text{Mg}^{2+}]_i$ , both  $B_{\Delta\text{Mg}}$  and  $[\text{Bu}]_i$  should increase toward infinity.

### Estimation of $B_{\Delta\text{Mg}}$ , $[\text{Bu}]_i$ , and $K_{\text{Bu}}$ from the present data

With  $7.57 \pm 5.23$  ( $n = 21$ ),  $B_{\Delta\text{Mg}}$  values calculated from the data presented here showed the variation expected from Fig. 7 A. In Fig. 7 B, the positions of the  $B_{\Delta\text{Mg}}$  values obtained in the present study are shown relative to the  $B_{\Delta\text{Mg}}$  calculated for an  $[\text{ATP}]_i$  of 5 mM. Although this  $[\text{ATP}]_i$  value corresponds to the top end of the range of  $[\text{ATP}]_i$  values obtained in leech Retzius neurons, all experimentally determined  $B_{\Delta\text{Mg}}$  values, irrespective of an inhibition of  $\text{Mg}^{2+}$  extrusion, lie considerably above the calculated  $B_{\Delta\text{Mg}}$  values, as denoted by the vertical projection of the measured values onto the calculated area (vertical lines in Fig. 7 B). In theory,  $\text{Mg}^{2+}$  buffering in Retzius neurons might be explained by an  $[\text{ATP}]_i$  of  $\sim 15$  mM, but such a value is considered to be unreasonably high. This indicates that even

if  $\text{Mg}^{2+}$  extrusion is blocked (Fig. 7 B),  $\text{Mg}^{2+}$  muffling in Retzius neurons cannot be solely explained by buffering through ATP.

For the calculation of the non-ATP muffling in Retzius neurons as  $[\text{Bu}]_i$  and  $K_{\text{Bu}}$ ,  $[\text{ATP}]_i$  was again assumed to be 5 mM.  $K_{\text{ATP}}$  was taken to be 0.117 mM (Lüthi et al. 1999; see Eq. 4). For  $\Delta[\text{Mg}]_i$  the mean value of 2.43 mM obtained during the iontophoretic  $\text{Mg}^{2+}$  injections was used, whereas the value of  $[\text{Mg}]_i$  was extrapolated from atomic absorption measurements of whole ganglia (F. Wolf and D. Günzel, unpublished data) and amounted to  $\sim 7$  mM. Using these values, a  $[\text{Bu}]_i$  of 7.5 mM and a  $K_{\text{Bu}}$  of 0.8 mM were obtained. A variation of  $[\text{ATP}]_i$  and  $[\text{Mg}]_i$  on the order of  $\pm 1$  mM resulted in a range of  $[\text{Bu}]_i$  values between 6.9 and 8.5 mM and in  $K_{\text{Bu}}$  values between 0.37 and 1.3 mM.

### Contribution of the $\text{Na}^+/\text{Mg}^{2+}$ antiport toward intracellular $\text{Mg}^{2+}$ muffling

The main indication that at least part of the intracellular  $\text{Mg}^{2+}$  muffling is due to  $\text{Mg}^{2+}$  extrusion via  $\text{Na}^+/\text{Mg}^{2+}$  antiport is the decrease in  $B_{\Delta\text{Mg}}$  observed in nominally  $\text{Na}^+$ -free bath solutions. Under these conditions  $\text{Na}^+/\text{Mg}^{2+}$  antiport, the major and to our knowledge sole  $\text{Mg}^{2+}$  extrusion mechanism in Retzius neurons, is inhibited (Günzel and Schlue, 1996). This inhibition is reflected by the sustained level in  $[\text{Mg}^{2+}]_i$  after  $\text{Mg}^{2+}$  injection in the absence of extracellular  $\text{Na}^+$  (Fig. 6 B).

However, even under these conditions of blocked  $\text{Mg}^{2+}$  extrusion, intracellular  $\text{Mg}^{2+}$  muffling is still considerably larger than would be expected from pure Mg-ATP buffering (Fig. 7 B), amounting to  $[\text{Bu}]_i$  values of 4.2 mM with a  $K_{\text{Bu}}$  of  $\sim 0.1$  mM. Thus, in the presence of extracellular  $\text{Na}^+$   $\sim 50\%$  of the observed non-ATP muffling is due to the action of  $\text{Na}^+/\text{Mg}^{2+}$  antiport.

### pH dependence of $[\text{Mg}^{2+}]_i$

Increases in  $[\text{Mg}^{2+}]_i$  observed during the initial phase of  $\text{H}^+$  injections into Retzius neurons were closely approximated by assuming ATP to be the sole intracellular buffer and using the relationship between pH and  $K_{\text{ATP}}$  for  $\text{Mg}^{2+}$  binding to ATP published by Lüthi et al. (1999) (Figs. 2 B and 3 B and Eq. 4). As expected from this relationship, injections of  $\text{OH}^-$  did not cause any changes in  $[\text{Mg}^{2+}]_i$  (Günzel et al., 1999). Initially, this finding appeared to contradict the previous finding that an intracellular alkalization induced by the application and subsequent removal of propionate caused release of  $\text{Mg}^{2+}$  from mitochondria and thus an increase in  $[\text{Mg}^{2+}]_i$  (Günzel et al., 1997, 1999). However, the trigger for  $\text{Mg}^{2+}$  release from mitochondria is not the cytoplasmic alkalization but an alkalization of the mitochondrial matrix (Petronilli et al., 1993), which may

be caused by the removal of propionate but not by OH<sup>-</sup> injection into the cytosol (Günzel et al., 1999).

In contrast to the effects of H<sup>+</sup> injections, it had to be deduced from the results of Mg<sup>2+</sup> injections into Retzius neurons that ATP is not the sole intracellular buffer (Fig. 7 B). Attempts were made to fit the experiment shown in Fig. 2 B while including additional, non-ATP Mg<sup>2+</sup> muffling. Under these conditions, the experimental data could be fitted only if either unrealistically high ATP concentrations (>10 mM) were used or if Mg<sup>2+</sup> binding to the non-ATP buffer showed a pH dependence similar to that of Mg<sup>2+</sup> binding to ATP.

It is therefore suggested that the amount of non-ATP Mg<sup>2+</sup> muffling is different during H<sup>+</sup> and Mg<sup>2+</sup> injection. On the one hand, H<sup>+</sup> injections caused an activation of the Na<sup>+</sup>/H<sup>+</sup> antiport and thus a rapid [Na<sup>+</sup>]<sub>i</sub> increase (Fig. 4) occurring equally in the presence and in the nominal absence of extracellular Mg<sup>2+</sup>. These [Na<sup>+</sup>]<sub>i</sub> increases reduced the driving force of the Na<sup>+</sup>/Mg<sup>2+</sup> antiport and thus caused a further increase in [Mg<sup>2+</sup>]<sub>i</sub> during the re-alkalinization of the neurons in the presence but not in the nominal absence of extracellular Mg<sup>2+</sup> (see Figs. 2 and 3). The effect of the acidification-induced [Na<sup>+</sup>]<sub>i</sub> increase on [Mg<sup>2+</sup>]<sub>i</sub> could be mimicked by [Na<sup>+</sup>]<sub>i</sub> increases elicited by the application of ouabain. Under these conditions only minor pH changes were observed, which have previously been shown to have no effect on [Mg<sup>2+</sup>]<sub>i</sub> (Günzel et al., 1997). On the other hand, pH<sub>i</sub> decreases may affect Mg<sup>2+</sup> uptake into mitochondria, as mitochondrial Mg<sup>2+</sup> transport has been found to be coupled to the H<sup>+</sup> gradient across the mitochondrial membrane (Jung and Brierley, 1994).

### Speculation on additional sources of [Mg<sup>2+</sup>]<sub>i</sub> muffling

The present results show that ~1/3 of Mg<sup>2+</sup> muffling in leech Retzius neurons is due to Mg<sup>2+</sup> binding to ATP, another 1/3 to extrusion. Thus, the source of ~30% of muffling is unknown. Part of it may be due to sequestration by mitochondria, as under certain conditions Mg<sup>2+</sup> can be released from mitochondria (Günzel et al., 1997) and therefore has to be taken up again at some point. The sum of all intracellular organic phosphates may also act as an intracellular Mg<sup>2+</sup> buffer. Due to a large volume/surface ratio, Mg<sup>2+</sup> binding to phospholipids of the cell membrane may not play an essential role in the soma of the neurons (Raftos et al., 1999) but might become important in neuronal axons and dendrites. Purely speculative, but probably worth considering in future, is the role of the cytoskeleton, namely of actin, as a Mg<sup>2+</sup> buffer. Under physiological conditions actin contains one Mg<sup>2+</sup> per monomer that is tightly bound ( $K_d$  0.1–1  $\mu$ M), but in addition there are five to nine low-affinity cation binding sites per monomer with  $K_d$  values of ~0.15 mM for Ca<sup>2+</sup> and Mg<sup>2+</sup> and ~10 mM for K<sup>+</sup> (Carrier et al., 1986). As the total actin concentration can

amount to 100–200  $\mu$ M (Korn et al. 1987), this would be equivalent to a binding site concentration of up to 2 mM. Actin therefore has to be expected to play a considerable role in Mg<sup>2+</sup> buffering.

## APPENDIX

### Calculation of intracellular Mg<sup>2+</sup> buffering

During iontophoretic injection of Mg<sup>2+</sup> into electrolyte droplets or cells the increase in the total Mg<sup>2+</sup> concentration,  $\Delta[\text{Mg}]_t$ , can be calculated from the following equation:

$$\Delta[\text{Mg}]_t = (\text{TI} \times I \times t) / (2 \times F \times V), \quad (1)$$

where TI is transport index,  $I$  is injection current,  $t$  is injection duration,  $F$  is Faraday constant, and  $V$  is droplet or cell volume. In experiments on electrolyte droplets  $\Delta[\text{Mg}]_t = \Delta[\text{Mg}]_{\text{dr}}$  if no Mg<sup>2+</sup> buffers are added to the electrolyte.

Cytoplasmic Mg<sup>2+</sup> muffling was calculated under the assumption that intracellular Mg<sup>2+</sup> binds to ATP and, in addition, is affected by various processes such as binding to unspecified intracellular binding sites, extrusion, or sequestration. The sum of these ATP-independent processes is described by a buffer equivalent (abbreviated Bu). All calculations are based on the following equations:

$$\begin{aligned} [\text{ATP}]_t &= [\text{ATP}]_i + [\text{MgATP}] \\ [\text{Bu}]_t &= [\text{Bu}]_i + [\text{MgBu}] \\ [\text{Mg}]_t &= [\text{Mg}^{2+}]_i + [\text{MgATP}] + [\text{MgBu}] \\ K_{\text{ATP}} &= [\text{Mg}^{2+}]_i \cdot [\text{ATP}]_i / [\text{MgATP}] \\ K_{\text{Bu}} &= [\text{Mg}^{2+}]_i \cdot [\text{Bu}]_i / [\text{MgBu}], \end{aligned}$$

where  $[\text{ATP}]_t$ ,  $[\text{Bu}]_t$ , and  $[\text{Mg}]_t$  denote the respective total concentrations;  $[\text{ATP}]_i$ ,  $[\text{Bu}]_i$ , and  $[\text{Mg}^{2+}]_i$  the respective free concentrations;  $[\text{MgATP}]$  and  $[\text{MgBu}]$  the concentrations of the complexes between Mg<sup>2+</sup> and ATP and Bu, respectively; and  $K_{\text{ATP}}$  and  $K_{\text{Bu}}$  the apparent dissociation constants of the binding between Mg<sup>2+</sup> and ATP and Bu, respectively.

$[\text{Mg}^{2+}]_i$  can be calculated from  $[\text{Mg}]_t$ ,  $[\text{ATP}]_t$ , and  $K_{\text{ATP}}$  using the following equation:

$$\begin{aligned} [\text{Mg}^{2+}]_i &= \frac{-(K_{\text{ATP}} + [\text{ATP}]_t - [\text{Mg}]_t)}{2} \\ &+ \sqrt{\frac{(K_{\text{ATP}} + [\text{ATP}]_t - [\text{Mg}]_t)^2}{4} + [\text{Mg}]_t K_{\text{ATP}}} \quad (2) \end{aligned}$$

If the effect of the buffer equivalent, Bu, is taken into consideration,  $[\text{Mg}^{2+}]_i$  becomes the positive, real solution of the cubic equation:

$$([\text{Mg}^{2+}]_i)^3 + A([\text{Mg}^{2+}]_i)^2 + B[\text{Mg}^{2+}]_i + C = 0, \quad (3)$$

with

$$\begin{aligned} A &= K_{\text{ATP}} + K_{\text{Bu}} + [\text{ATP}]_t + [\text{Bu}]_t - [\text{Mg}]_t \\ B &= K_{\text{ATP}} \times K_{\text{Bu}} + [\text{ATP}]_t \times K_{\text{Bu}} + [\text{Bu}]_t \\ &\quad \times K_{\text{ATP}} - [\text{Mg}]_t \times K_{\text{ATP}} - [\text{Mg}]_t \times K_{\text{Bu}} \\ C &= -[\text{Mg}]_t \times K_{\text{ATP}} \times K_{\text{Bu}}. \end{aligned}$$



$K_{ATP}$  shows a pH dependence that has recently been described by the following relationship (Lüthi et al., 1999):

$$K_{ATP}(pH) = \frac{102.006(1 + 10^{(6.484-pH)})}{1 + 0.0325 \times 10^{(6.484-pH)}} \quad (4)$$

The muffling ratio,  $B_{\Delta Mg}$ , was defined as  $\Delta[Mg]_i/\Delta[Mg^{2+}]_i$  in analogy to Schwiening and Thomas (1996). If  $Mg^{2+}$  is buffered only by ATP,  $B_{\Delta Mg}$  can be expressed as

$$B_{\Delta Mg} = \frac{\Delta[Mg]_i}{\Delta[Mg^{2+}]_i} = 1 + \frac{[ATP]_i K_{ATP}}{(K_{ATP} + [Mg^{2+}]_i + \Delta[Mg^{2+}]_i)(K_{ATP} + [Mg^{2+}]_i)} \quad (5)$$

For infinitesimal  $\Delta[Mg]_i$  and  $\Delta[Mg^{2+}]_i$ ,  $B_{\Delta Mg}$  approaches the buffering coefficient,  $B_{Mg}$ , which was defined as  $d[Mg]_i/d[Mg^{2+}]_i$  by Koss et al. (1993) and which can be expressed as

$$B_{Mg} = \frac{d[Mg]_i}{d[Mg^{2+}]_i} = 1 + \frac{[ATP]_i \times K_{ATP}}{(K_{ATP} + [Mg^{2+}]_i)^2} \quad (6)$$

If, in addition to ATP, there is assumed to be the  $Mg^{2+}$  buffer equivalent, Bu, Eq. 5 has to be extended to

$$B_{\Delta Mg} = 1 + \frac{[ATP]_i K_{ATP}}{(K_{ATP} + [Mg^{2+}]_i + \Delta[Mg^{2+}]_i)(K_{ATP} + [Mg^{2+}]_i)} + \frac{[Bu]_i K_{Bu}}{(K_{Bu} + [Mg^{2+}]_i + \Delta[Mg^{2+}]_i)(K_{Bu} + [Mg^{2+}]_i)} \quad (7)$$

We express our thanks to Dr. F. Wolf (Rome, Italy) and Dr. J. Schumann (Düsseldorf, Germany) for carrying out the AAS measurements of  $[Mg]_i$  and the ATP assay, respectively.

Supported by Ministerium für Forschung und Wissenschaft, Nordrhein-Westfalen.

## REFERENCES

- Atkins, P. W. 1994. Physical Chemistry, 5th ed. Oxford University Press, Oxford.
- Belan, P., P. Kostyuk, V. Snitsarev, and A. Tepikin. 1993. Calcium clamp in isolated neurons of the snail *Helix pomatia*. *J. Physiol.* 462:47–58.
- Carlier, M.-F., D. Pantaloni, and E. D. Korn. 1986. Fluorescence measurements of the binding of cations to high-affinity and low-affinity sites on ATP-G-actin. *J. Biol. Chem.* 261:10778–10784.
- Csernoch, L., J. C. Bernengo, P. Szentesi, and V. Jacquemond. 1998. Measurement of intracellular  $Mg^{2+}$  concentration in mouse skeletal muscle fibers with the fluorescent indicator Mag-Indo-1. *Biophys. J.* 75:957–967.
- Dierkes, P. W., S. Neumann, A. Müller, D. Günzel, and W.-R. Schlue. 2001. Simultaneous measurement of cell volume, membrane potential and intracellular ion concentrations in invertebrate nerve cells by multi-barreled ion-selective microelectrodes. In *Electrochemical Microsystem Technologies*. T. Osaka, M. Datta, and J. W. Schultze, editors. Gordon and Breach, Tokyo. In press.
- Flatman, P. W. 1988. The effects of magnesium and potassium transport in ferret red blood cells. *J. Physiol.* 397:471–487.
- Flatman, P. W., and V. L. Lew. 1980. Magnesium buffering in intact human red blood cells measured using the ionophore A23187. *J. Physiol.* 305:13–30.
- Freudenrich, C. C., E. Murphy, L. A. Levy, R. E. London, and M. Lieberman. 1992. Intracellular pH modulates cytosolic free magnesium in cultured chicken heart cells. *Am. J. Physiol.* 262:C1024–C1030.
- Fry, C. H., S. K. Hall, L. A. Blatter, and J. A. S. McGuigan. 1990. Analysis and presentation of intracellular measurements obtained with ion-selective microelectrodes. *Exp. Physiol.* 75:187–198.
- Grubbs, R. D., and A. Walter. 1994. Determination of cytosolic  $Mg^{2+}$  activity and buffering in BC<sub>3</sub>H-1 cells with mag-fura2. *Mol. Cell. Biochem.* 136:11–22.
- Günther, T., J. Vormann, and R. Averdunk. 1986. Characterization of furosemide-sensitive  $Mg^{2+}$  influx in Yoshida ascites tumor cells. *FEBS Lett.* 197:297–300.
- Günther, T., J. Vormann, and J. A. S. McGuigan. 1995. Buffering and activity coefficient of intracellular free magnesium concentration in human erythrocytes. *Biochem. Mol. Biol. Int.* 37:871–875.
- Günzel, D., S. Durry, and W.-R. Schlue. 1997. Intracellular alkalization causes  $Mg^{2+}$  release from intracellular binding sites in leech Retzius neurons. *Pflügers Arch.* 435:65–73.
- Günzel, D., A. Müller, S. Durry, and W.-R. Schlue. 1999. Multi-barreled ion-sensitive microelectrodes and their application in micro-droplets and biological systems. *Electrochim. Acta.* 44:3785–3793.
- Günzel, D., and W.-R. Schlue. 1996. Sodium/magnesium antiport in Retzius neurons of the leech *Hirudo medicinalis*. *J. Physiol.* 491:595–608.
- Günzel, D., and W.-R. Schlue. 1997. Interactions between magnesium, sodium and intracellular pH in leech Retzius neurons. In *Advances in Magnesium Research*. R. Smetana, editor. J. Libbey, London. 498–507.
- Günzel, D., F. Zimmermann, and W.-R. Schlue. 1998. Estimation of the  $Mg^{2+}$  buffering capacity in leech Retzius neurons. In *Proceedings of the 26th Göttingen Neurobiology Conference*. N. Elsner and R. Wehner, editors. Thieme Verlag, Stuttgart. 620.
- Hintz, K., D. Günzel, and W.-R. Schlue. 1999.  $Na^+$ -dependent regulation of the free  $Mg^{2+}$  concentration in neuropile glial cells and P neurons of the leech *Hirudo medicinalis*. *Pflügers Arch.* 437:354–362.
- Jung, D. W., and G. P. Brierley. 1994. Magnesium transport by mitochondria. *J. Bioenerg. Biomembr.* 26:527–535.
- Kato, H., H. Gotoh, M. Kajikawa, and K. Suto. 1998. Depolarization triggers intracellular magnesium surge in cultured dorsal root ganglion neurons. *Brain Res.* 779:329–333.
- Korn, E. D., M.-F. Carlier, and D. Pantaloni. 1987. Actin polymerization and ATP hydrolysis. *Science*. 238:638–644.
- Koss, K. L., and R. D. Grubbs. 1994. Elevated extracellular  $Mg^{2+}$  increases  $Mg^{2+}$  buffering through a Ca-dependent mechanism in cardiomyocytes. *Am. J. Physiol.* 267:C633–C641.
- Koss, K. L., R. W. Putnam, and R. D. Grubbs. 1993.  $Mg^{2+}$  buffering in cultured chick ventricular myocytes: quantitation and modulation by  $Ca^{2+}$ . *Am. J. Physiol.* 264:C1259–C1269.
- Leonhard-Marek, S., G. Gabel, and H. Martens. 1998. Effects of short chain fatty acids and carbon dioxide on magnesium transport across sheep rumen epithelium. *Exp. Physiol.* 83:155–164.
- Li, H. Y., and G. A. Quamme. 1994. Effect of pH on intracellular  $Mg^{2+}$  in isolated adult rat cardiomyocytes. *Biochim. Biophys. Acta.* 1222:164–170.
- Lipton, P. 1999. Ischemic cell death in brain neurons. *Physiol. Rev.* 79:1431–1568.
- Lüthi, D., D. Günzel, and J. A. S. McGuigan. 1999. Mg-ATP binding: its modification by spermine, the relevance to cytosolic  $Mg^{2+}$  buffering, changes in the intracellular ionized  $Mg^{2+}$  concentration and the estimation of  $Mg^{2+}$  by  $^{31}P$ -NMR. *Exp. Physiol.* 84:231–252.
- Müller, A., D. Günzel, and W.-R. Schlue. 1997. Effect of kainate on  $[Mg^{2+}]_i$ ,  $[Na^+]_i$ , pH<sub>i</sub> and  $E_m$  in leech Retzius neurons investigated using multi-barreled microelectrodes. In *Proceedings of the 25th Göttingen Neurobiology Conference*. N. Elsner and H. Wässle, editors. Thieme Verlag, Stuttgart. 799.



- Neher, E. 1995. The use of fura-2 for estimating Ca buffers and Ca fluxes. *Neuropharmacology*. 34:1423–1442.
- Petronilli, V., C. Cola, and P. Bernardi. 1993. Modulation of the mitochondrial cyclosporin A-sensitive permeability transition pore. II. The minimal requirements for pore induction underscore a key role for transmembrane electrical potential, matrix pH, and matrix  $\text{Ca}^{2+}$ . *J. Biol. Chem.* 268:1011–1016.
- Pissarek, M., C. Reichelt, G.-J. Krauss, and P. Illes. 1998. Tolbutamide attenuates diazoxide-induced aggravation of hypoxic cell injury. *Brain Res.* 812:164–171.
- Plaschke, K., E. Matrin, and H. J. Bardenheuer. 1998. Effect of propentofylline on hippocampal brain energy state and amyloid precursor protein concentration in a rat model of cerebral hypoperfusion. *J. Neural Transm.* 105:1065–1077.
- Rajdev, S., and I. J. Reynolds. 1995. Calcium influx but not pH or ATP level mediates glutamate induced changes in intracellular magnesium in cortical neurons. *J. Neurophysiol.* 74:942–949.
- Raftos, J. E., V. L. Lew, and P. W. Flatman. 1999. Refinement and evaluation of a model of  $\text{Mg}^{2+}$  buffering in human red cells. *Eur. J. Biochem.* 263:635–645.
- Romani, A., and A. Scarpa. 1992. Regulation of cell magnesium. *Arch. Biochem. Biophys.* 298:1–12.
- Scharrer, E., and T. Lutz. 1990. Effects of short chain fatty acids and K on absorption of Mg and other cations by the colon and caecum. *Z. Ernährungswiss.* 29:162–168.
- Schlue, W.-R., and J. W. Deitmer. 1980. Extracellular potassium in neuropile and nerve cell body region of the leech central nervous system. *J. Exp. Biol.* 87:23–43.
- Schlue, W.-R., and R. C. Thomas. 1985. A dual mechanism for intracellular pH regulation by leech neurons. *J. Physiol.* 364:327–338.
- Schwiening, C. J., and R. C. Thomas. 1996. Relationship between intracellular calcium and its muffling measured by calcium iontophoresis in snail neurons. *J. Physiol.* 491:621–633.
- Siesjö, B. K., and S. C. Sørensen. 1971. Quantification of “buffering” in vivo. In *Ion Homeostasis of the Brain*. B. K. Siesjö and S. C. Sørensen, editors. Academic Press, New York. 457–464.
- Strothmann, H., K. Kiefer, and R. Altvater-Mackensen. 1986. Equilibration of the ATPase reaction of chloroplasts at transition from strong light to weak light. *Biochim. Biophys. Acta.* 850:90–96.
- Thomas, R. C., J. A. Coles, and J. W. Deitmer. 1991. Homeostatic muffling. *Nature*. 350:564.
- Westerblad, H., and D. G. Allen. 1992. Myoplasmic free  $\text{Mg}^{2+}$  concentration during repetitive stimulation of single fibres from mouse skeletal muscle. *J. Physiol.* 453:413–434.